

An artificial synapse capable of regulating signal transmission speed in a neuromorphic network

Jingru Sun(孙晶茹), Xiaosong Li(李晓崧), Yichuang Sun(孙义闯), Zining Xiong(熊子宁), and Jiqi He(何计奇)
Citation: Chin. Phys. B, 2026, 35 (**1**): 010501. DOI: 10.1088/1674-1056/ae1c2c
http://cpb.iphy.ac.cn; http://iopscience.iop.org/cpb

What follows is a list of articles you may be interested in

A sound-sensitive neuron incorporating a memristive-ion channel

Xin-Lin Song(宋欣林), Ge Zhang(张鬲), and Fei-Fei Yang(杨飞飞)
Chin. Phys. B, 2025, 34 (**12**): 120502. DOI: 10.1088/1674-1056/ae0563

Design of a memristive chaotic map and its adaptive regulation

Ya Wang(王亚), Xin-Lin Song(宋欣林), and Fei-Fei Yang(杨飞飞)
Chin. Phys. B, 2025, 34 (**9**): 090504. DOI: 10.1088/1674-1056/adea5c

Firing activities in a fractional-order Hindmarsh-Rose neuron with multistable memristor as autapse

Zhi-Jun Li(李志军), Wen-Qiang Xie(谢文强), Jin-Fang Zeng(曾金芳), and Yi-Cheng Zeng(曾以成)
Chin. Phys. B, 2023, 32 (**1**): 010503. DOI: 10.1088/1674-1056/ac65f7

Effect of astrocyte on synchronization of thermosensitive neuron-astrocyte minimum system

Yi-Xuan Shan(单仪萱), Hui-Lan Yang(杨惠兰), Hong-Bin Wang(王宏斌), Shuai Zhang(张帅), Ying Li(李颖), and Gui-Zhi Xu(徐桂芝)
Chin. Phys. B, 2022, 31 (**8**): 080507. DOI: 10.1088/1674-1056/ac490c

Langevin approach with rescaled noise for stochastic channel dynamics in Hodgkin-Huxley neurons

Huang Yan-Dong (黄艳东), Li Xiang (李翔), Shuai Jian-Wei (帅建伟)
Chin. Phys. B, 2015, 24 (**12**): 120501. DOI: 10.1088/1674-1056/24/12/120501

SPECIAL TOPIC — Biophysical circuits: Modeling & applications in neuroscience

An artificial synapse capable of regulating signal transmission speed in a neuromorphic network

Jingru Sun(孙晶茹)[1,†], Xiaosong Li(李晓崧)[1], Yichuang Sun(孙义闯)[2], Zining Xiong(熊子宁)[1], and Jiqi He(何计奇)[1]

[1] *College of Computer Science and Electronic Engineering, Hunan University, Changsha* 410082, *China*
[2] *The School of Engineering and Computer Science, University of Hertfordshire, Hatfield AL*10 9*AB, UK*

(Received 1 July 2025; revised manuscript received 5 November 2025; accepted manuscript online 6 November 2025)

The regulation of signal transmission speed is one of the most important capabilities of the biological nervous system. This study explores the mechanisms and methods for regulating signal transmission speed among nonmyelinated neurons within the same brain region, starting from spike-timing-dependent plasticity (STDP) of synapses. Building upon the Hodgkin–Huxley model, the dynamic behavior of synapses is incorporated, and the adaptive growth neuron (AGN) model is proposed. Artificial synaptic structures and neuronal physical nodes are also designed. The artificial synaptic structure exhibits unidirectionality, memory capacity, and STDP, enabling it to connect neuronal physical nodes through branching and merging structures. Furthermore, the artificial synapse can adjust signal transmission speed, regulate functional competition between different regions of the neuromorphic network, and promote information interaction. The findings of this study endow neuromorphic networks with the ability to regulate signal transmission speed over the long term, providing new insights into the development of neuromorphic networks.

Keywords: artificial synapse, neuromorphic networks, Hodgkin–Huxley model, neuron circuit, memristor, neurodynamics

PACS: 05.45.–a, 87.19.lg, 87.19.ll

DOI: 10.1088/1674-1056/ae1c2c **CSTR:** 32038.14.CPB.ae1c2c

1. Introduction

With the continuous iteration of hardware devices and artificial intelligence (AI) algorithms, the data-processing capabilities of deep learning algorithms are constantly improving. Large models, such as ChatGPT, Sora, and V-JEPA, have surpassed the human brain in speed and accuracy when processing standardized large-scale data.[1–4] However, as shown in Fig. 1, due to limitations in computational architectures, deep learning algorithms lack the ability to regulate signal transmission speed and to achieve efficient information synchronization, which is fundamental to the brain's creativity, generalization ability, and coordination.[5,6] Consequently, deep learning algorithms are far inferior to the brain in terms of innovation and environmental adaptation. Neuromorphic networks transmit and process information through spike sequences, and their structures and operating principles are very similar to those of the biological nervous system.[7] Compared with deep learning algorithms, they have greater potential to realize the brain's advantageous capabilities.

Regulating signal transmission speed is crucial for the complex, time-varying dynamic information synchronization of the biological brain. According to functional organization, the brain hemispheres are divided into 52 regions, which are connected to other regions, either directly or indirectly, through neurons, forming a complex network. The transmission of commands or the processing of sensory information requires close cooperation among multiple regions, which demands timely sharing and transmission of information between these regions.[8,9] However, the demand for information interaction speed between brain regions is not fixed and continuously changes according to the content of the task being processed.[10,11] To ensure timely synchronization of information between brain regions, the biological nervous system has evolved the ability to regulate signal transmission speed.

Artificial synapses are mainly used in neuromorphic networks, and due to differences in the types of neuromorphic networks, the design focus of synapses varies. According to design approaches, neuromorphic networks are primarily categorized into two main types: those motivated by artificial neural networks (ANNs) and those motivated by natural neuronal networks (NNNs).[12–16]

The first category of neuromorphic networks focuses on converting ANNs into spiking neural networks (SNNs), using neuromorphic chips designed with leaky integrate-and-fire (LIF) neuron nodes to perform ANN algorithms.[17–21] For ANNs, changing synaptic weights affects the computational load rather than the signal transmission speed. In neuromorphic chips, changes in synaptic weights are achieved through memory elements such as memristors or electrolyte-

[†]Corresponding author. E-mail: jt_sunjr@hnu.edu.cn

© 2026 Chinese Physical Society and IOP Publishing Ltd. All rights, including for text and data mining, AI training, and similar technologies, are reserved.

gated transistors (EGTs).[22–24] Although this approach significantly reduces the power consumption of ANN algorithms, these synapses still cannot regulate signal transmission speed. Their functionality and precision remain essentially comparable to those of ANN algorithms.

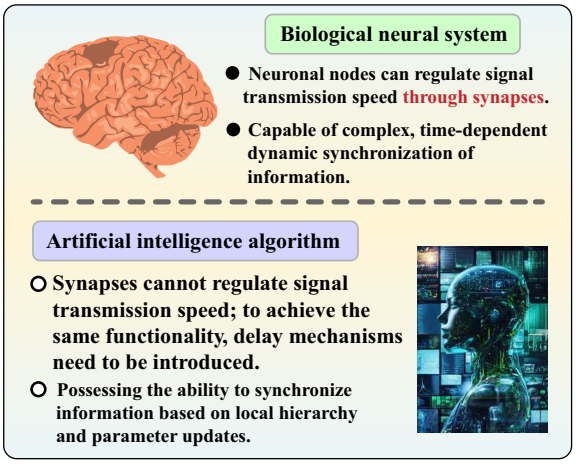


Fig. 1. Comparison between the biological nervous system and AI algorithms.

For the second type of neuromorphic network, greater emphasis is placed on the reverse implementation of the brain's physiological functions, aiming to replicate the functions of biological neurons, synapses, and network structures as accurately as possible. Existing studies on biological neurons have demonstrated that synaptic delay is not constant; instead, it can be modulated by factors such as the presynaptic action potential waveform, release probability, or physiological conditions, thereby optimizing the timing of information transmission through neural circuits.[25,26] In recent years, several studies have treated delay as a tunable parameter and incorporated it into models, demonstrating significant improvements in performance or reductions in weight precision requirements for certain temporal tasks.[27] Such approaches are typically implemented at the software or simulation level by employing trainable delays or by mimicking delay learning through architectural mechanisms such as dilated convolutions or sparse selection. At the hardware level, however, mapping delay parameters onto controllable properties of synaptic devices or circuit components, such as triggering thresholds, RC time constants, or local delay elements, remains an active yet challenging research direction.

Therefore, this paper begins with an examination of the physiological structures of biological neurons and synapses, referencing the dynamic behavior of neuronal spike firing and the biological mechanisms underlying synaptic weight changes, and then designs an artificial synapse. The artificial synapse is capable of spike-timing-dependent plasticity (STDP) and of adjusting signal transmission speed. The main contributions of this paper are as follows.

(i) This study designs excitatory and inhibitory artificial synapse structures based on biological mechanisms and the dynamic behaviors of synaptic weight changes. The artificial synapses are equipped with STDP.

(ii) The Hodgkin–Huxley (HH) model is extended to incorporate the dynamic behavior of excitatory and inhibitory synapses, and a neuronal circuit node is designed. The node can adjust the firing rate by modifying synaptic weights or stimulus types, thereby accelerating signal transmission and processing in neuromorphic networks.

(iii) Based on the aforementioned neuronal circuit nodes, a straightforward neuromorphic network is constructed to analyze the effects of synaptic weight changes on signal transmission speed, information synchronization between brain regions, and competition for functional dominance among brain regions.

This paper is organized as follows. Section 2 introduces STDP in synapses, with a focus on the design of excitatory and inhibitory synapses. Section 3 integrates synaptic dynamics into the HH model, proposing the adaptive generative neuron (AGN) model and detailing the designs of artificial synapses and neuronal nodes. Section 4 verifies the unidirectionality, memory capacity, and STDP of these artificial structures. Section 5 evaluates branching and merging connection methods through experiments. Section 6 examines how artificial synapses control signal transmission speed, synchronize information, and prioritize neuronal activity. Section 7 concludes the paper.

2. Necessary biological background knowledge

Understanding the mechanisms of synaptic weight changes and the dynamic behavior of biological synapses is crucial for enabling artificial synapses to exhibit more biological characteristics. This section mainly introduces the biological principles and explanations underlying changes in synaptic weights.

2.1. Excitatory synapse

Excitatory synapses enhance or promote signal transmission by releasing excitatory neurotransmitters, such as glutamate. Their primary function is to depolarize the postsynaptic neuron (i.e., raise the membrane potential), making it more likely to generate an action potential. STDP of excitatory synapses conforms to the description of Hebb's rule. Long-term potentiation (LTP) and long-term depression (LTD) are the primary manifestations of STDP. The timing interval and the firing order of spikes generated by pre- and postsynaptic neurons are the primary factors determining whether synaptic connections undergo LTP or LTD.[28–31] In the field of neuroscience, a time window of 10–100 ms is widely recognized.[32–34] If the presynaptic neuron fires a

spike first and the postsynaptic neuron fires a spike within this time window, the synaptic weight increases, which is known as LTP. The opposite holds for LTD. Long-term synaptic plasticity is primarily achieved through changes in the number and density of α-amino-3-hydroxy-5-methyl-4-isoxazolepropionic acid (AMPA) receptor ion channels on the postsynaptic membrane. An increase in the number and density of AMPA receptor channels enhances channel conductivity, thereby elevating synaptic weight, whereas a decrease has the opposite effect. The concentration of Ca^{2+} in the postsynaptic terminal determines the synthesis and degradation of AMPA receptor ion channels.[30]

LTP: As shown in Fig. 2(a), AMPA and N-methyl-D-aspartate (NMDA) receptor ion channels are embedded in the postsynaptic membrane. Positive ions, such as Na^+ and Ca^{2+}, from outside the cell enter the neuron through these channels, generating postsynaptic currents that stimulate neuronal firing. NMDA receptors are primarily Ca^{2+}-selective channels that are normally blocked by Mg^{2+}. Therefore, even when bound to neurotransmitters, positive ions cannot pass through them into the neuron. When AMPA receptors bind to neurotransmitters and are activated, Na^+ enters the cell along a concentration gradient. This causes the membrane potential (MP) of the neuron to rise, repelling the Mg^{2+} that blocks the NMDA receptor and allowing Ca^{2+} to enter the cell in large quantities. An increase in intracellular calcium concentration, together with a spike-timing interval of 10–100 ms, stimulates the postsynaptic neuron to synthesize new AMPA receptor ion channels, thereby increasing synaptic weight.[35]

LTD: As shown in Fig. 2(b), the primary difference between the triggers for LTD and LTP lies in the firing order of the pre- and postsynaptic neurons. For LTD, the postsynaptic neuron fires first. When it receives neurotransmitters released by the presynaptic neuron, it is still in a hyperpolarized state or in the process of returning to its resting membrane potential. The postsynaptic current entering the cell through AMPA receptor ion channels cannot raise the MP sufficiently to repel the Mg^{2+} that blocks NMDA receptor ion channels. Therefore, Ca^{2+} cannot enter the cell effectively. When the concentration of Ca^{2+} inside the postsynaptic neuron is low, AMPA receptor ion channels are degraded, thereby reducing synaptic weight.[31]

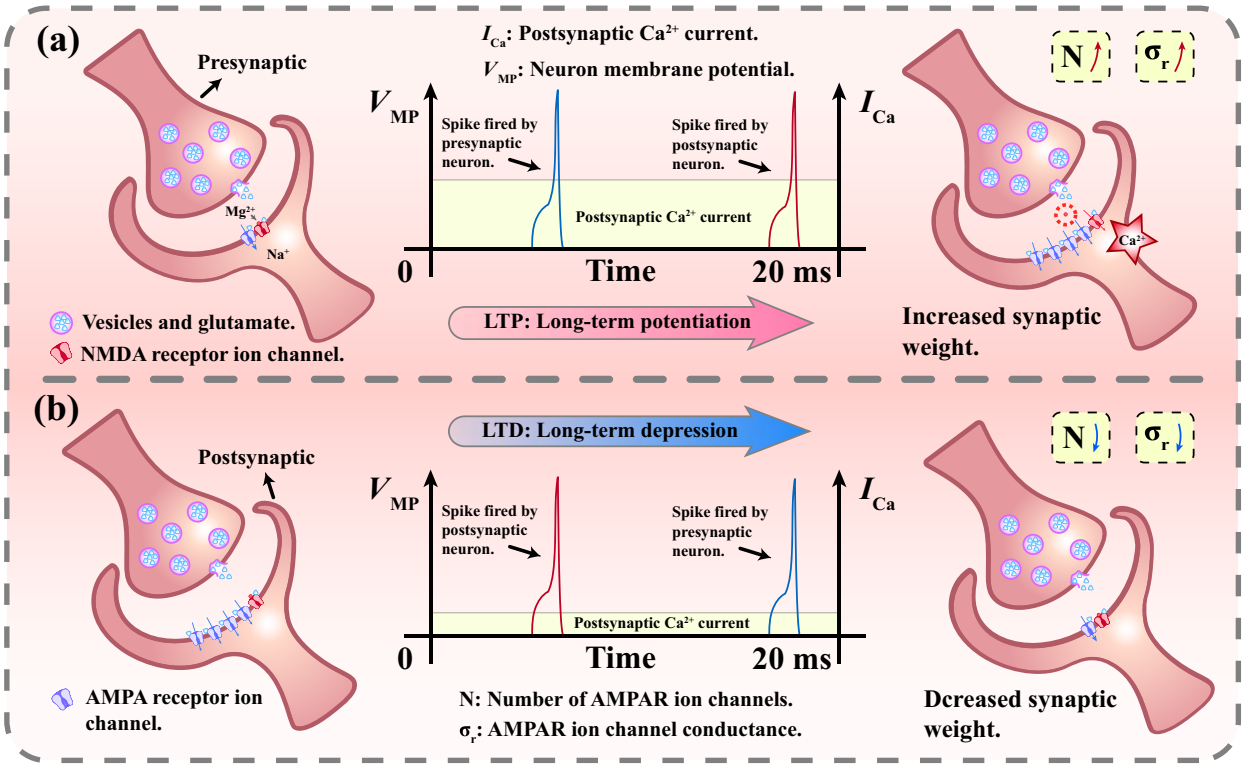


Fig. 2. Physiological mechanisms of LTP and LTD. (a) LTP, (b) LTD.

2.2. Inhibitory synapse

Inhibitory synapses reduce or suppress signal transmission by releasing inhibitory neurotransmitters such as γ-aminobutyric acid (GABA) or glycine. Their primary function is to hyperpolarize (i.e., decrease the membrane potential of) the postsynaptic neuron, making it less likely to generate an action potential. In the brain, inhibitory synapses account for about 20%, and compared with excitatory synapses, synaptic weight changes in inhibitory synapses are more complex and less well studied. Inhibitory synapses exhibit inhibitory long-term potentiation (iLTP) and inhibitory long-term depression (iLTD), with synaptic weight changes reflected in variations

in the number of $GABA_A$ receptor ion channels on the postsynaptic membrane. At present, related studies have only demonstrated that changes in inhibitory synaptic weights are associated with factors such as the duration of low-frequency stimulation, Ca^{2+} concentration, and growth and development. The detailed transcriptional and hydrolytic mechanisms of $GABA_A$ receptors still require further investigation.

3. Synapses, neuron circuit nodes, and their dynamics

This section introduces the physical replacements for key neuronal organelles, the AGN model derived from the extended HH model, and the neuronal circuit physical node.

3.1. Physical replacement of organelles

The physical alternatives for each ion channel are shown in Fig. 3(a). The main organelles involved in neuronal spike discharge behavior include AMPA receptor ion channels, Na^+ and K^+ channels, and the cell membrane. The dynamic characteristics of memristors are remarkably similar to the biological properties of ion channels, making them a preferred choice for the physical replacement of neuronal ion channels.[35–37] According to their activation modes, these ion channels can be classified into three categories.

3.2. Inhibitory synapse

Inhibitory synapses reduce or suppress signal transmission by releasing inhibitory neurotransmitters such as GABA or glycine. Their primary function is to hyperpolarize (i.e., decrease the membrane potential of) the postsynaptic neuron, making it less likely to generate an action potential. In the brain, inhibitory synapses account for about 20%, and compared with excitatory synapses, synaptic weight changes in inhibitory synapses are more complex and less well studied. Inhibitory synapses exhibit iLTP and iLTD, with synaptic weight changes reflected in variations in the number of $GABA_A$ receptor ion channels on the postsynaptic membrane. At present, related studies have only demonstrated that changes in inhibitory synaptic weights are associated with factors such as the duration of low-frequency stimulation, Ca^{2+} concentration, and growth and development. The detailed transcriptional and hydrolytic mechanisms of $GABA_A$ receptors still require further investigation.

The first category consists of non-voltage-gated leak ion channels, as indicated by R_T in Fig. 3(a). Myelination, by structurally forming insulating sheaths and nodes of Ranvier, functionally enables a significant increase in signal transmission speed, a reduction in energy consumption, and an enhancement of information reliability, thereby serving as a critical foundation for efficient neural communication. Without considering neuronal myelination, these ion channels can be emulated using fixed resistors to achieve their biological functions. The cell membrane is replaced with a conventional capacitor when myelination is not considered. Since this study mainly focuses on the effect of synapses on signal transmission speed, both the experimental and theoretical analyses are conducted with the degree of myelination fixed, specifically with $R_T = 2\ \text{k}\Omega$ and $C = 1\ \mu\text{F}$.

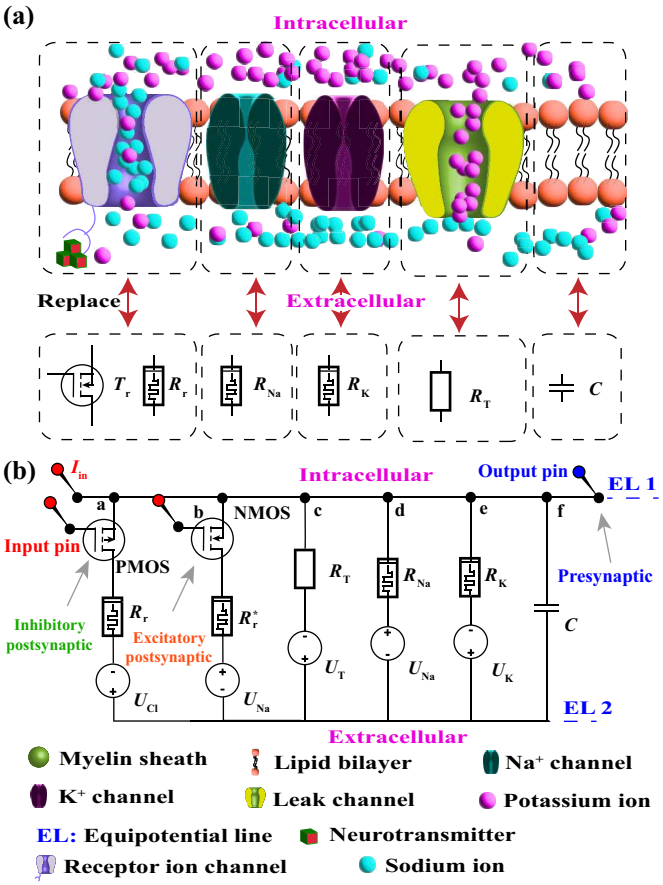


Fig. 3. (a) Physical replacements for each ion channel. (b) Schematic diagram of the neuronal circuit physical node.

The second type comprises voltage-gated ion channels, represented by Na^+ and K^+ channels. High-speed, single-compartment memristors can reproduce the physiological functions of such ion channels.[35,37] The models of Na^+ and K^+ channel memristors discussed in this paper are derived from Refs. [35,36,38].

The third category consists of chemically gated ion channels, represented by AMPA or $GABA_A$ receptor ion channels. The activation of this type of ion channel does not depend on changes in membrane potential but requires binding with neurotransmitters. Therefore, memristors, which are two-terminal devices, are unsuitable for simulating their functions. Currently, the devices that most closely mimic the biological characteristics of this type of ion channel are EGTs.[23,24] However, their ability to maintain stable resistance states still requires further verification. Therefore, this paper adopts a combination of memristors and transistors, namely a 1T1M structure, to simulate AMPA or $GABA_A$ receptor ion channels, as

shown in branch 'a' of Fig. 3(b). For excitatory synapses, the dynamics of memristor R_r are described by Eqs. (1)–(4). Due to the lack of consensus on the biological mechanisms and dynamic behaviors of inhibitory synaptic weight changes in neuroscience, this paper only provides the structural design of inhibitory artificial synapses and does not involve the design of memristors R_r^* that satisfy iLTP and iLTD.

$$V(t) = (R_{\text{off}} - x \cdot \Delta R) \cdot i(t), \tag{1}$$

$$\frac{\mathrm{d}x}{\mathrm{d}t} = \begin{cases} -k_{\text{on}}^{b_1} \cdot a_1 \cdot (1 - x^{2p}) \cdot i(t) \cdot \Delta R, \\ V_{\text{th1}} \le V(t), \quad x_2(t) > V_{\text{th3}}, \\ k_{\text{off}}^{b_2} \cdot a_2 \cdot [1 - (x-1)^{2p}] \cdot i(t) \cdot \Delta R, \\ V_{\text{th2}} \ge V(t), \quad x_3(t) > V_{\text{th4}}, \end{cases} \tag{2}$$

$$x_2(t) = \begin{cases} (a_3) \cdot R^* \cdot \left(1 - \exp\left(-\dfrac{t - t_0}{R^* \cdot C^*}\right)\right), \\ V(t) < V_{\text{th2}}, \quad V(t_0) = V_{\text{th2}}, \\ (b_3) \cdot R^* \cdot \left(1 - \exp\left(-\dfrac{t - t_1}{R^* \cdot C^*}\right)\right), \\ V(t) \ge V_{\text{th2}}, \quad V(t_0) = V_{\text{th2}}, \end{cases} \tag{3}$$

$$x_3(t) = \begin{cases} (a_4) \cdot R^* \cdot \left(1 - \exp\left(-\dfrac{t - t_0}{R^* \cdot C^*}\right)\right), \\ V(t) > V_{\text{th1}}, \quad V(t_0) = V_{\text{th1}}, \\ (b_4) \cdot R^* \cdot \left(1 - \exp\left(-\dfrac{t - t_1}{R^* \cdot C^*}\right)\right), \\ V(t) \le V_{\text{th1}}, \quad V(t_0) = V_{\text{th1}}, \end{cases} \tag{4}$$

where $V(t)$ represents the real-time potential difference across the terminals of the memristor; R_{off} and R_{on} represent the resistances of the memristor in the high-resistance and low-resistance states, respectively; and ΔR denotes the absolute difference between them. The variable x represents the resistance change coefficient, and $i(t)$ denotes the real-time current flowing through the memristor. Parameters a_1, b_1, a_2, b_2, p, k_{off}, and k_{on} are adjustment parameters that control the variation speed and nonlinear characteristics of x. V_{th1}, V_{th2}, V_{th3}, and V_{th4} are the operating thresholds of the memristor. Variables $x_2(t)$ and $x_3(t)$ are activation functions that satisfy the Hebbian rule. Parameters a_3, b_3, a_4, b_4, R^*, and C^* are model coefficients.

3.3. Dynamics of AGN

Due to concentration differences of various ions inside and outside neurons, multiple Nernst potentials are formed across the neuronal membrane. As shown in Fig. 3(b), V_{Na} and V_{K} represent the Nernst potentials generated by the concentration gradients of Na^+ and K^+, respectively, with values of 55 mV and −77 mV. Branch 'b' realizes the function of leak channels, that is, the biological characteristics of non-voltage-gated, always-open K^+ channels. Therefore, the value of V_{T} is approximately equal to V_{K}, namely −71 mV. Ions flowing through AMPA receptor ion channels are primarily Na^+; therefore, the value of V_{r} is equal to V_{Na}. Equation (5) describes the dynamics of the AGN.

$$I(t) = I_{\text{c}}(t) + \sum_k I_k(t), \tag{5}$$

where $I_{\text{c}}(t)$ and $I_k(t)$ correspond to the capacitive current and the real-time ionic currents flowing through ion channels, respectively. $I(t)$ represents the real-time total current through the axonal cell membrane. Because of myelination and membrane potential variations, $I_{\text{c}}(t)$ can be further expressed as

$$I_{\text{c}}(t) = \frac{C(t) \cdot \mathrm{d}u}{\mathrm{d}t}, \tag{6}$$

where $C(t)$ represents the real-time membrane capacitance, and $\frac{\mathrm{d}u}{\mathrm{d}t}$ denotes the rate of change of the membrane potential. $C(t)$ is determined by the dynamic equation of the voltage-gated capacitor.[15] The real-time currents flowing through each ion channel are given by

$$\begin{aligned} \sum_k I_k(t) \;=\; & g_{\text{Na}}(t) \cdot (u - V_{\text{Na}}) + g_{\text{K}}(t) \cdot (u - V_{\text{K}}) \\ & + g_{\text{r}}(t) \cdot (u - V_{\text{Na}}) + g_{\text{r}}^*(t) \cdot (u - V_{\text{Cl}}) \\ & + g_{\text{T}}(t) \cdot (u - V_{\text{T}}), \end{aligned} \tag{7}$$

where $g_{\text{Na}}(t)$, $g_{\text{K}}(t)$, $g_{\text{r}}(t)$, $g_{\text{r}}^*(t)$, and $g_{\text{T}}(t)$ represent the real-time conductances of the ion channel memristors shown in Fig. 3(b), with values determined by the corresponding memristor dynamic equations. V_{Na}, V_{K}, V_{T}, and V_{Cl} correspond to the Nernst potentials generated by ionic concentration gradients. The variable u represents the real-time membrane potential of the neuron.

Synapses primarily regulate signal transmission speed by modulating the instantaneous firing frequency of neuronal spikes. Therefore, based on the neuron model, this study investigates the relationship between synaptic weight and instantaneous firing frequency. Since the activation of inhibitory synapses suppresses neuronal spiking, the analysis primarily focuses on excitatory synaptic inputs. As illustrated in Fig. 4, an increase in excitatory synaptic weight (i.e., a higher conductance g_{r}) leads to an increase in the instantaneous firing frequency, thereby accelerating neural signal transmission.

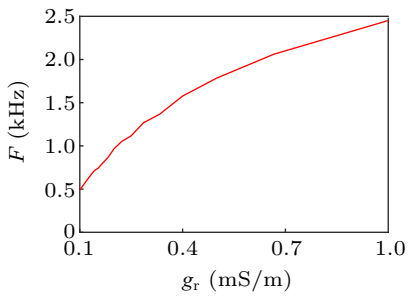


Fig. 4. Relationship between synaptic weight and the instantaneous firing frequency of neuronal output spikes.

4. Simulation

Through simulation of the neuronal circuit physical node, the unidirectional transmission, the impact of synaptic weight changes, and the STDP behavior of the artificial synapse structure are validated. The simulation is based on PSpice.

4.1. Verification of unidirectional signal transmission

Unidirectional signal transmission refers to the phenomenon whereby the firing of a postsynaptic neuron does not affect the membrane potential of the presynaptic neuron. Unidirectionality clarifies the transmission target, prevents reverse signal interference, and supports the hierarchical organization of complex networks. Specifically, unidirectionality facilitates independent adjustment of synaptic weights, thereby enabling the learning and memory capabilities of neural networks. Unidirectionality is an inherent characteristic of neural networks, and synapses, serving as communication bridges between neurons, must ensure unidirectional signal transmission. Both excitatory and inhibitory synapses transmit signals via receptor ion channels.[39] Therefore, testing the unidirectionality of the receptor ion channel circuit can serve as an indirect verification of whether the corresponding excitatory and inhibitory synapse circuits possess unidirectional signal transmission properties.

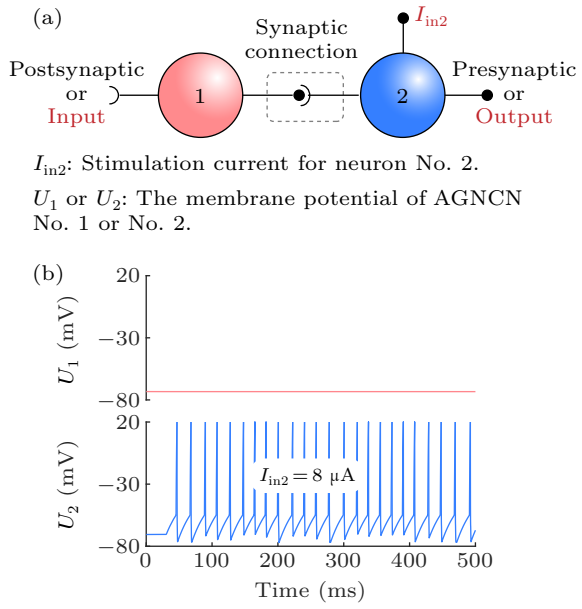


Fig. 5. (a) Neuron connection scheme in the synaptic unidirectional transmission verification experiment. (b) Simulation results of unidirectionality verification.

As shown in Fig. 5(a), a short chain consisting of two neurons is designed. By applying input current stimulation ($I_{in2} > 0$, corresponding to excitatory stimulation) to the postsynaptic neuron No. 2 to induce it to fire spike trains, while observing the membrane potential changes of the presynaptic neuron No. 1, it is possible to determine whether the artificial synapse exhibits unidirectionality.

As illustrated by the simulation results in Fig. 5(b), the input current stimulation causes postsynaptic neuron No. 2 to fire a high-frequency spike train. In contrast, the membrane potential of presynaptic neuron No. 1 remains unchanged. The results demonstrate that the membrane potential of presynaptic neuron No. 1 is independent of whether postsynaptic neuron No. 2 fires spikes, directly verifying that the artificial synapse structure possesses the capability for unidirectional signal transmission. As shown in Fig. 3(b), the structures of excitatory and inhibitory synapses are identical, with the differences lying in their corresponding Nernst potentials and transistors. Therefore, verifying that the artificial synaptic structure possesses unidirectional transmission is sufficient, and there is no need to verify excitatory and inhibitory artificial synapses separately.

4.2. Verification of impact of synaptic weight changes

Whether synaptic weight changes can affect the firing characteristics of neurons is a key issue in the design of artificial synapses, and this must be validated before verifying STDP. Similar to the verification of unidirectionality, since the structure of the artificial synapse is the same, there is no need to separately verify the impact of weight changes for excitatory and inhibitory artificial synapses. Subsequent simulations therefore still take the excitatory artificial synapse structure as an example.

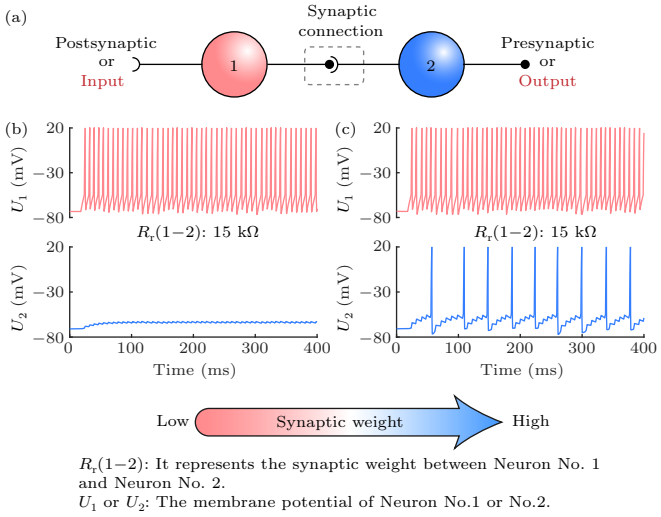


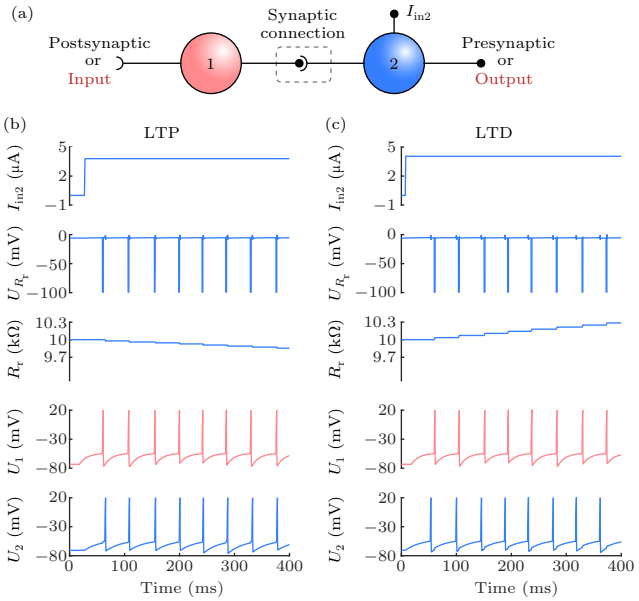
Fig. 6. (a) Neuron connection scheme for verifying synaptic weight changes. (b) Simulation results of synaptic weight change verification.

As shown in Fig. 6(a), an artificial excitatory synapse connects two neuron circuit nodes. By applying constant stimulation to induce neuron No. 1 to fire spikes at a fixed frequency, the weight of the artificial synapse is adjusted, and the membrane potential changes of neuron No. 2 are observed to verify whether synaptic weight changes affect neuronal information transmission. The simulation results are shown in Fig. 6(b). When the weight of the artificial synapse is relatively low

($R_r(1-2) = 15$ kΩ), the constant output of neuron No. 1 only causes oscillations in the membrane potential of neuron No. 2. However, when the weight increases ($R_r(1-2) = 5$ kΩ), the constant output of neuron No. 1 can induce neuron No. 2 to fire spikes. These simulation results demonstrate that changes in the weight of the artificial synapse can strengthen or weaken the influence of presynaptic neuron No. 1 on the firing characteristics of postsynaptic neuron No. 2. This indicates that the weight adjustment mechanism in the artificial synapse structure proposed in this study can effectively alter signal transmission pathways within the neuromorphic network.

4.3. Verification of STDP in artificial excitatory synapses

As mentioned earlier, due to the lack of conclusive research in modern neuroscience regarding the biological mechanisms and dynamic behavior of inhibitory synapses, this study could not design memristors to fully realize the iLTP and iLTD characteristics of inhibitory synapses. Therefore, only the verification of STDP in artificial excitatory synapses is provided here. As shown in Fig. 7(a), two neuron circuit nodes are connected by an artificial excitatory synapse. In this setup, the AMPA receptor ion channels of the presynaptic neuron No. 1 are set to be closed, causing the neuron to emit spikes continuously at a fixed frequency. Following Hebbian's law, the precise timing of the excitatory stimulus input to the postsynaptic neuron No. 2 controls whether the postsynaptic neuron emits spikes before or after the presynaptic neuron. Under the condition that Hebbian's law is satisfied, the synaptic weight change of the artificial synapse is carefully observed to verify whether it exhibits STDP. Simulation results are shown in Figs. 7(b) and 7(c).



U_1 or U_2: The membrane potential of neuron No.1 or No.2.
I_{in2}: Current stimulation for neuron No. 2.
R_r: Synaptic weight between Neuron No. 1 and No. 2.

Fig. 7. (a) Neuron connection scheme for verifying STDP; (b) LTP of synapses; (c) LTD of synapses.

Comparing U_1 and U_2 in Fig. 7(b), within the window period, the presynaptic neuron No. 1 fires before the postsynaptic neuron No. 2, satisfying the condition for LTP. As R_r decreases, the synaptic weight increases, indicating that the artificial synapse exhibits LTP characteristics similar to those of biological synapses. A smaller R_r corresponds to a larger artificial synaptic weight. This important conclusion can be drawn by comparing the results shown in Figs. 6(b) and 6(c). Comparing U_1 and U_2 in Fig. 7(c), during the window period, the postsynaptic neuron No. 2 fires before the presynaptic neuron No. 1, satisfying the condition for LTD. As R_r continuously increases, the synaptic weight decreases, indicating that the artificial synapse exhibits LTD characteristics similar to those of biological synapses. After satisfying Hebbian's law, the artificial excitatory synapse can undergo long-term potentiation or long-term depression, clearly demonstrating that it exhibits STDP.

5. Physical experiment

After verifying unidirectionality and STDP, it is necessary to verify whether the artificial synapse structure can support branching or merging connections.

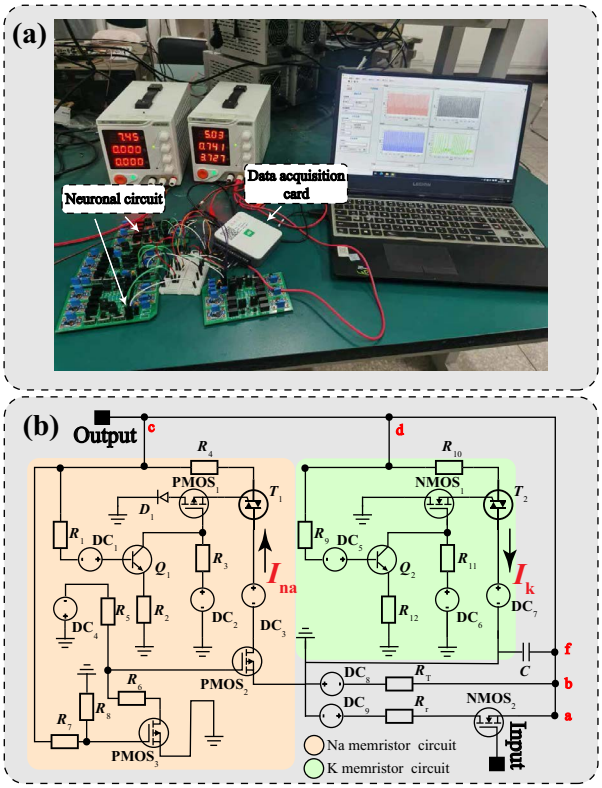


Fig. 8. (a) Physical experiment setup. (b) Equivalent circuit of Na^+ and K^+ channel memristors.

5.1. Physical experiment setup

The physical experiment setup is shown in Fig. 8(a). To collect continuous spike sequences, a signal acquisition platform is built based on an NI acquisition card (model USB-

6002), with the sampling rate set to 50000 Hz, which fully covers the frequency variation range of the spike sequences. The neuron circuit is constructed as shown in Fig. 3(b), and the Na^+ and K^+ channel memristors are replaced by equivalent circuits. The equivalent circuits of the Na^+ and K^+ channel memristors are shown in Fig. 8(b).

5.2. Physical experiment and result analysis

As shown in Figs. 9(a) and 9(b), four neurons are connected to verify the branching and merging connection functionalities of artificial synapses. The physical experiment results for branching and merging are shown in Figs. 10(a) and 10(b). In the branching experiment results shown in Fig. 10(a), due to the different synaptic weights between presynaptic neuron No. 1 and postsynaptic neurons No. 2, No. 3, and No. 4, only postsynaptic neuron No. 4 successfully emitted action potentials. However, the membrane potentials of postsynaptic neurons No. 2 and No. 3 also exhibited varying degrees of oscillation. The information carried by the presynaptic neuron was successfully transmitted through the artificial synapse structure to the postsynaptic neurons via three separate pathways.

In the merging experiment results shown in Fig. 10(b), postsynaptic neuron No. 4 successfully integrated the information carried by presynaptic neurons No. 1, No. 2, and No. 3 through the artificial synapses, expressing it in the form of an irregular spike sequence. The results of the branching and merging physical experiments demonstrate that the artificial synapse structure designed in this study can be used to construct complex neuromorphic networks.

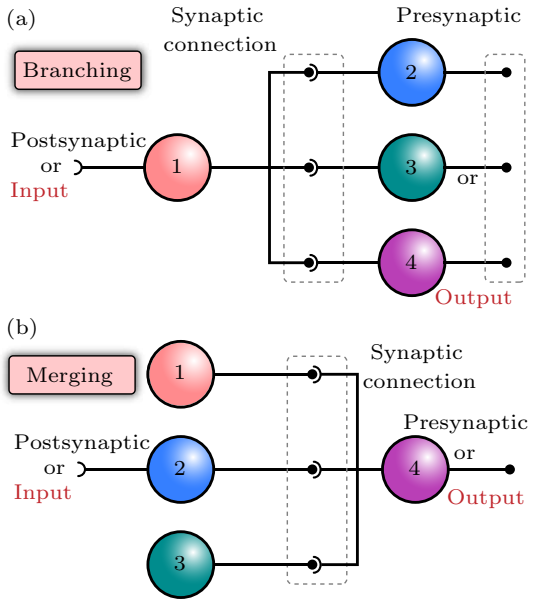


Fig. 9. (a) Branching connections in neuronal circuits. (b) Merging connections in neuronal circuits.

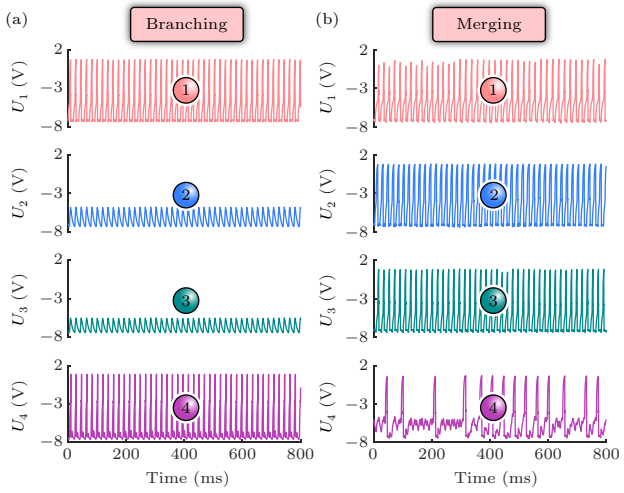


Fig. 10. (a) Branching connections in neuronal circuits. (b) Merging connections in neuronal circuits.

6. Advanced functional properties of artificial synapses in neuromorphic networks

The previous sections have validated the unidirectionality, STDP, and branching and merging functions of the artificial synapse structure proposed in this study. Existing artificial synapses include the features mentioned above, but biological synapses possess many additional functions. Next, we discuss three aspects in more detail: signal transmission speed regulation, information synchronization, and priority control.

6.1. Regulation of signal transmission speed through excitatory synaptic modulation

The brain recruits neurons to form neural clusters with specific functions to complete related tasks. Neurons within the cluster require high-frequency interactions. Due to the close spatial distance between neurons, most information transmission relies on unmyelinated neurons. In the cellular structure of unmyelinated neurons, synapses play a role in regulating the speed of signal transmission. Therefore, we have incorporated the function of controlling signal transmission speed into the design of artificial synapses. This can be verified through a three-neuron link, as shown in Fig. 11. In the experiment, neuron No. 1 generates spikes at a fixed frequency, as shown in Figs. 12(a) and 12(b). By adjusting the synaptic weights between neuron No. 1, neuron No. 2, and neuron No. 3, the time at which neuron No. 3 fires its first spike is recorded. This allows us to determine whether the artificial synapse can regulate the signal transmission speed.

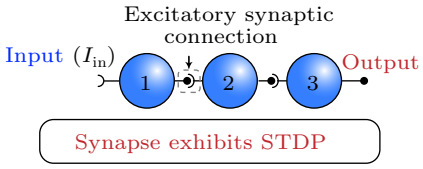


Fig. 11. Verification of artificial synapses in regulating signal transmission speed in a neuromorphic link.

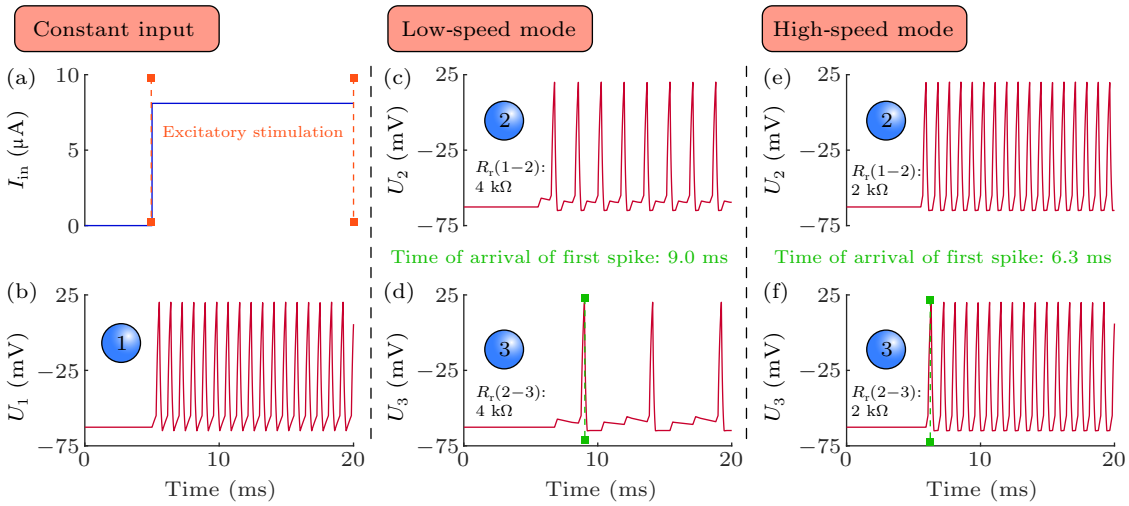


Fig. 12. Experimental results verifying the regulation of signal transmission speed by the artificial synapse in a neuromorphic link. (a) Excitatory input to neuron No. 1; (b) output spikes of neuron No. 1; (c) output spikes of neuron No. 2 when $R_r(1-2) = 4$ kΩ; (d) output spikes of neuron No. 3 when $R_r(2-3) = 4$ kΩ; (e) output spikes of neuron No. 2 when $R_r(1-2) = 2$ kΩ; (f) output spikes of neuron No. 3 when $R_r(2-3) = 2$ kΩ.

As shown in Figs. 12(c) and 12(d), in the low-speed mode, when the synaptic weight is low (with larger $R_r(1-2)$ and $R_r(2-3)$), the first spike from neuron No. 3 occurs at 9 ms. In the high-speed mode, as shown in Figs. 12(e) and 12(f), when the synaptic weight is higher (with smaller $R_r(1-2)$ and $R_r(2-3)$), the first spike from neuron No. 3 occurs at 6.3 ms. By adjusting the synaptic weight, the time for the signal to travel from neuron No. 1 to neuron No. 3 is reduced by 2.7 ms, indicating that the artificial synapse structure proposed in this study can effectively regulate signal transmission speed in neuromorphic networks.

It is important to note that synaptic regulation of transmission speed applies primarily to shorter transmission links, whether in biological neural systems or neuromorphic networks. This is because changes in synaptic weight alter the magnitude of the postsynaptic membrane current, leading to a large influx of cations into the cell in a short time. As a result, more energy is required to restore the neuron to its original ionic concentration balance after firing. Increasing the postsynaptic membrane current in biomimetic neural circuit nodes also leads to higher energy consumption.[40,41] Therefore, myelinated biomimetic neural circuit nodes should still be used to reduce energy consumption when adjusting the transmission speed for long-link communication.

6.2. Synaptic mechanisms for information synchronization across brain regions

The timely sharing of signals between brain regions is the foundation for cooperation among different brain regions, and the signal regulation function of synapses plays a crucial role in this process. As shown in Fig. 13, assume that brain region No. 1 receives a signal and, after processing it, needs to simultaneously transmit the information to brain region No. 3 and brain region No. 4 for further processing. However, the signal fired by brain region No. 1 must be processed by brain region No. 2 before it can be transmitted to brain region No. 3. Therefore, compared to the neuronal pathway between brain region No. 1 and brain region No. 3 (neuron No. 1 to neuron No. 3), the neuronal pathway between brain region No. 1 and brain region No. 4 (neuron No. 1 to neuron No. 4) has one less neuron. By adjusting the weights of the artificial synapses, the signals can reach brain region No. 3 and brain region No. 4 almost simultaneously, meeting the requirement for information synchronization between brain regions. This can be demonstrated through a simple experiment.

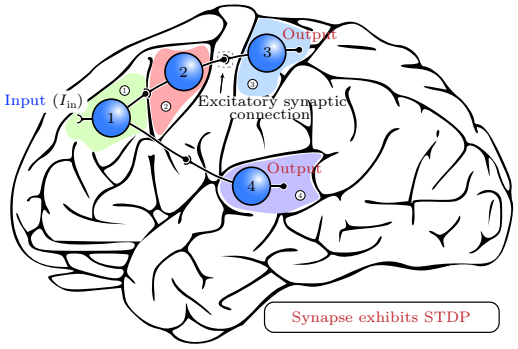
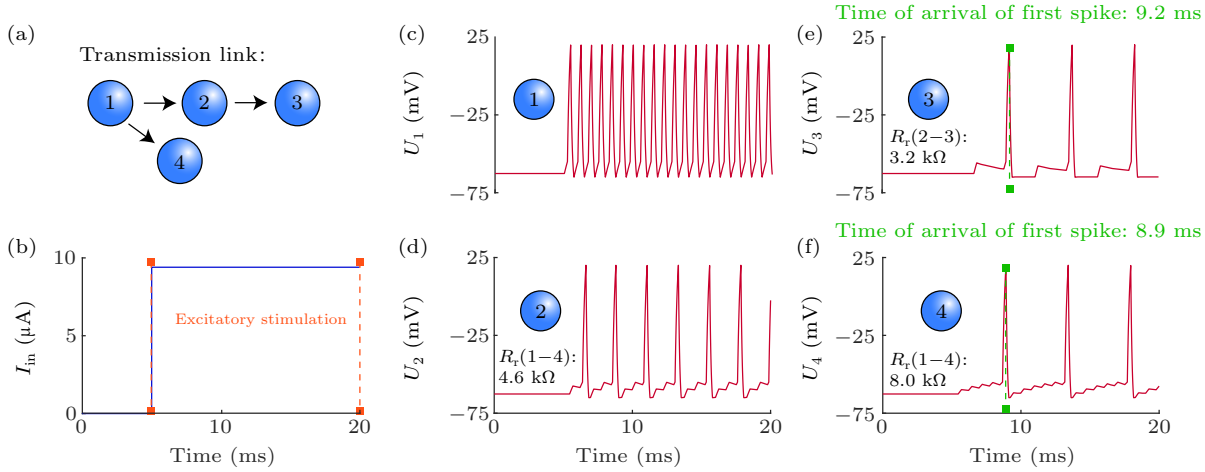


Fig. 13. Conceptual diagram of information synchronization across brain regions.

The four neurons are connected according to the structure shown in Fig. 14(a). As shown in Figs. 14(b) and 14(c), under constant excitatory stimulation, neuron No. 1 emits spikes at a fixed frequency. For the first pathway, the signal is generated by neuron No. 1, passes through neuron No. 2, and is transmitted to neuron No. 3. The moment neuron No. 3 fires its first spike is at 9.2 ms. For the second pathway, the signal is generated by neuron No. 1 and directly reaches neuron No. 4. The moment when neuron No. 4 emits its first spike

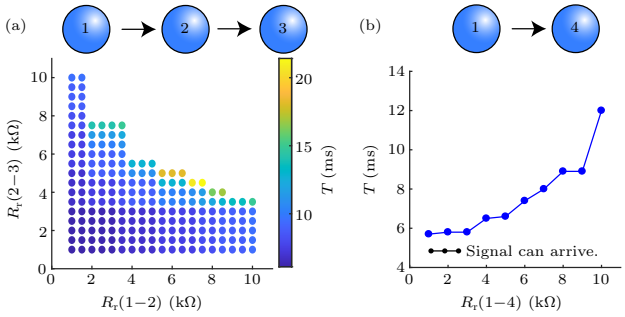
is at 8.9 ms. The signals almost simultaneously reach neuron No. 3 and neuron No. 4.

The relationship between the synaptic weights of the two signal transmission pathways and the times at which the signals reach the endpoints is shown in Fig. 15. For the path from neuron No. 1 to neuron No. 3, the weights $R_r(1-2)$ and $R_r(2-3)$ are adjusted to control the signal transmission speed, as shown in Fig. 15(a). For the pathway from neuron No. 1 to neuron No. 4, adjusting the weight $R_r(1-4)$ controls the signal transmission speed, as shown in Fig. 15(b). The relationship between synaptic weights and the times it takes for signals to reach the endpoints of different pathways demonstrates that, even with varying transmission routes and distances, adjusting synaptic weights can synchronize signal arrival times at the endpoints, achieving information synchronization.



$R_r(1-2)$ represents the synaptic weight between Neuron No. 1 and Neuron No. 2.
$R_r(2-3)$ represents the synaptic weight between Neuron No. 2 and Neuron No. 3.
$R_r(1-4)$ represents the synaptic weight between Neuron No. 1 and Neuron No. 4.

Fig. 14. Results of the information synchronization experiment across brain regions. (a) Two neuronal pathways. (b) Excitatory input to neuron No. 1. (c) Output spikes of neuron No. 1. (d) Output spikes of neuron No. 2. (e) Output spikes of neuron No. 3. (f) Output spikes of neuron No. 4.



T (ms): The moment when the signal reaches the endpoint.

Fig. 15. Relationship between synaptic weights and signal transmission time to endpoints. (a) Path from neuron No. 1 to neuron No. 3. (b) Path from neuron No. 1 to neuron No. 4.

6.3. Inhibitory synapses for functional competition and priority control among brain regions

The previous sections have discussed and verified most of the characteristics of artificial excitatory synapses. This section will introduce the function of inhibitory synapses. Functional competition between brain regions refers to the dynamic interaction where different brain regions compete for resources, attention, or processing time to perform various cognitive tasks. This competition can arise when multiple brain regions are involved in processing different tasks simultaneously, leading to the need for the brain to prioritize certain functions over others. In this case, inhibitory synapses can regulate which brain regions are most active or dominant at any given time, helping to manage competition and ensuring the priority of critical functions while minimizing interference between competing processes. An experiment can be conducted to demonstrate how artificial inhibitory synapses help manage functional competition and priority control between brain regions.

As shown in Fig. 16(a), when a person or animal is subjected to a sudden intense stimulus or injury, the instinctive response is to avoid it. However, as shown in Fig. 16(b), a person can consciously control their limbs to endure harm, which involves regulating the brain and inhibitory synapses. As shown in Fig. 16(c), assume brain region No. 1 receives and processes pain information, brain region No. 2 generates the idea and controls the limb to endure the harm, and brain region No. 3 controls the limb to avoid harm. When a person is subconscious and suddenly experiences a strong stimulus or injury, brain region No. 1 receives the pain information. It sends the processed result to brain region No. 3, causing the person to avoid harm.

However, when a person intends to endure harm, it is first necessary to prevent the function of brain region No. 3 from taking effect. At this point, brain region No. 2, through inhibitory synapses, suppresses the neurons in brain region No. 3

from generating action potentials, making it impossible for the person to avoid harm. In this process, brain region No. 2 has a higher priority than brain region No. 3, as its activation suppresses the function of brain region No. 3. As shown in Figs. 17(a) and 17(b), constant excitatory input is used to induce neuron No. 1 (corresponding to brain region No. 1) to emit spikes at a fixed frequency, simulating pain signals. As shown in Figs. 17(c) and 17(d), in a subconscious state, neuron No. 2 (corresponding to brain region No. 2) does not generate action potentials. In contrast, neuron No. 3 (corresponding to brain region No. 3) generates action potentials and successfully begins avoiding harm at 7.7 ms.

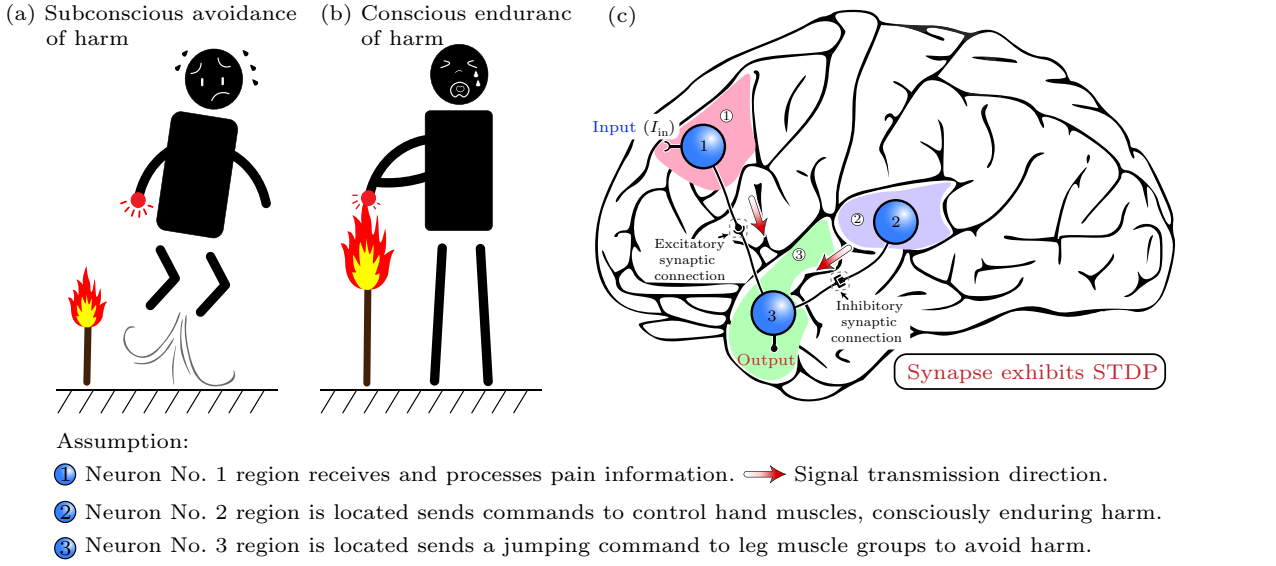


Fig. 16. Functional competition among brain regions. (a) In a subconscious state, the body actively avoids harm with minimal brain involvement. (b) Under conscious control, the body endures harm. (c) Functional competition and priority control among brain regions.

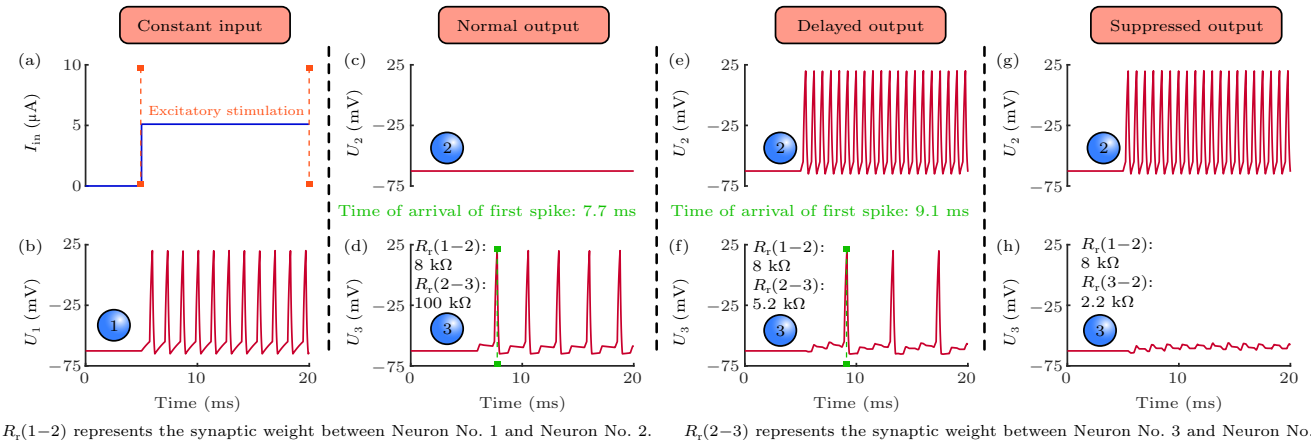


Fig. 17. Experimental results of functional competition and priority regulation among brain regions. (a) Excitatory input stimulus to neuron No. 1. (b) Spikes output by neuron No. 1. (c) Neuron No. 2 output in the subconscious avoidance state; (d) neuron No. 3 output in the subconscious avoidance state; (e) neuron No. 2 output in the delayed avoidance scenario; (f) neuron No. 3 output in the delayed avoidance scenario; (g) neuron No. 2 output when actively enduring harm; (h) neuron No. 3 output when actively enduring harm.

There are two scenarios for consciously enduring harm: delaying harm avoidance actions and continuously enduring the harm. As shown in Figs. 17(e) and 17(f), for the first scenario, the artificial inhibitory synapse weight is low ($R_r(2-3) = 5.2$ kΩ), and the action potentials fired by neuron No. 2 cannot completely suppress the spikes from neuron No. 3. neuron No. 3 fires a spike at 9.1 ms, delayed by 1.4 ms compared to the subconscious state. As shown in Figs. 17(g) and 17(h), for the second scenario, the artificial inhibitory synapse weight is higher ($R_r(2-3) = 2.2$ kΩ). The action potentials emitted by neuron No. 2 completely suppress the spikes from neuron No. 3, allowing the active endurance of harm. Neuron No. 2 emits a spike, causing neuron No. 3 to either delay or not emit a spike. At this point, the function of brain region No. 2 dominates, verifying the role of inhibitory synapses in functional competition and priority regulation between brain regions. In addition, inhibitory synapses can prevent neurons from becoming excessively excited, helping to avoid neurological disorders such as epilepsy, which are caused by abnormal neuronal discharge.

7. Conclusion

In this study, we propose artificial excitatory and inhibitory synaptic structures and verify most of the physiological functions that synapses should possess. In particular, we provide a detailed discussion on the role of artificial synapses in regulating signal transmission speed, information synchronization, functional competition, and priority control between brain regions in a neuromorphic network. First, starting from the physiological structure of biological synapses, we discuss the STDP of excitatory and inhibitory synapses and design artificial excitatory and inhibitory synaptic structures. Next, based on the HH model, we incorporate the dynamic behavior descriptions of excitatory and inhibitory synapses, propose the AGN model, and design the corresponding physical node. Finally, experiments are conducted to verify the artificial synapses' unidirectionality, STDP, and branching and merging connection methods. The experiments demonstrate that artificial synapses can regulate signal transmission speed in a neuromorphic network, synchronize information across different regions promptly, and control functional competition and priority among various regions.

Information synchronization and priority control of functional regions are crucial for the smooth operation of robotic movements. In the future, further exploration will be conducted on the physiological functions of excitatory and inhibitory synapses to improve the design of artificial synapses. At the same time, the relationship between synaptic regulation of signal transmission speed and energy consumption will be further investigated. These advancements will be applied to robotic motion control systems while providing a theoretical foundation for the further development of neuromorphic networks.

Acknowledgments

This project was supported by the National Natural Science Foundation of China (Grant No. 62171182), the Natural Science Foundation Project of Hunan Province (Grant No. 2025JJ50345), and the Postgraduate Scientific Research Innovation Project of Hunan Province (Grant No. CX20240452).

References

[1] Asemi A, Asemi A, Ko A and Alibeigi A 2022 *J. Big Data* **9** 13
[2] Yang S, Wang H, Pang Y, Azghadi M R and Linares-Barranco B 2024 *IEEE Trans. Biomed. Circuits Syst.* **18** 186
[3] Chen J, Park S, Popovski P, Poor H V and Simeone O 2024 *IEEE Trans. Signal Process.* **72** 4635
[4] Greco D, Osborne F, Pusceddu S and Reforgiato Recupero D 2025 *J. Big Data* **12** 64
[5] Courellis H S, Minxha J, Cardenas A R, Kimmel D L, Reed C M, Valiante T A, Salzman C D, Mamelak A N, Fusi S and Rutishauser U 2024 *Nature* **632** 841
[6] Collins K M, Sucholutsky L, Bhatt U, Chandra K, Wong L, Lee M, Zhang C E, Tan Z, Ho M, Mansinghka V, Weller A, Tenenbaum J B and Griffiths T L 2024 *Nat. Hum. Behav.* **8** 1851
[7] Saranirad V, Dora S, McGinnity T M and Coyle D 2025 *IEEE Trans. Neural Netw. Learn. Syst.* **36** 2274
[8] Dorkenwald S, Matsliah A, Sterling A R, *et al.* 2024 *Nature* **634** 124
[9] Peng H, Xie P, Liu L, *et al.* 2021 *Nature* **598** 174
[10] Wang J, Meng F, Xu C, Zhang Y, Liang K, Han C, Gao Y, Yu X, Li Z, Zeng X, Ni J, Tan H, Yang J and Ma Y 2024 *Nat. Neurosci.* **28** 161
[11] Andrade-Talavera Y, Fisahn A and Rodríguez-Moreno A 2023 *Mol. Psychiatry* **28** 2177
[12] Li X, Sun J, Sun Y, Wang C, Hong Q, Du S and Zhang J 2024 *IEEE Trans. Circuits Syst. I Regul. Pap.* **71** 2320
[13] Pickett M D, Medeiros-Ribeiro G and Williams R S 2013 *Nat. Mater.* **12** 114
[14] Yi W, Tsang K K, Lam S K, Bai X, Crowell J A and Flores E A 2018 *Nat. Commun.* **9** 4661
[15] Li X, Sun J, Ma W, Sun Y, Wang C and Zhang J 2024 *IEEE Trans. Consum. Electron.* **70** 3669
[16] Ham D, Park H, Hwang S and Kim K 2021 *Nat. Electron.* **4** 635
[17] Ma M and Lu Y 2024 *Chaos* **34** 033116
[18] Priyanka T M C, Vignesh D, Gowrisankar A, *et al.* 2025 *Eur. Phys. J. Plus* **140** 363
[19] Sanjeet S, Sahoo B D and Parhi K K 2024 *IEEE Trans. Circuits Syst. Artif. Intell.* **1** 149
[20] Xiao P, Du S, Wei Z, Hong Q and Wen S 2024 *IEEE Trans. Circuits Syst. Artif. Intell.* **1** 272
[21] Tu H, Luo Y, Zeng K, Wu Y, Zhang L, Zhang B and Zeng Z 2023 *Chin. Phys. B* **32** 107504
[22] Yu F, Su D, He S, Wu Y, Zhang S and Yin H 2025 *Chin. Phys. B* **34** 050502
[23] Peng Y, Wu H, Gao B, Tang J, Zhang Q, Zhang W, Yang J J and Qian H 2020 *Nature* **577** 641
[24] Lian X J, Fu J K, Gao Z X, Gu S P and Wang L 2023 *Chin. Phys. B* **32** 017304
[25] Shang C, Sun K and Wang Z H S 2023 *Nonlinear Dyn.* **111** 20347
[26] Zhang W, Gao B, Tang J, Yao P, Yu S, Chang M, Yoo H, Qian H and Wu H 2020 *Nat. Electron.* **3** 371
[27] Ling H, Koutsouras D A, Kazemzadeh S, van de Burgt Y, Yan F and Gkoupidenis P 2020 *Appl. Phys. Rev.* **7** 011307
[28] Lee H, Cho J, Jin M, Lee J H, Lee C, Kim J, Lee J, Shin J C, Yoo J, Lee E and Kim Y S 2024 *ACS Nano* **18** 5383
[29] Ben-Ari Y, Khazipov R, Leinekugel X, Caillard O and Gaiarsa J L 1997 *Trends Neurosci.* **20** 523
[30] Boudkkazi S, Fronzaroli-Molinieres L and Debanne D 2011 *J. Physiol.* **589** 1117
[31] Lin J W and Faber D S 2002 *Trends Neurosci.* **25** 449
[32] Li Y, Gan J, Lin X, Qiu Y, Zhan H and Tian H 2024 *IEEEACM Trans. Audio, Speech, Lang. Process.* **32** 2814
[33] Li S, McLaughlin D W and Zhou D 2023 *Commun. Pure Appl. Math.* **76** 114
[34] Markram H, Lübke J, Frotscher M and Sakmann B 1997 *Science* **275** 213
[35] Bi G Q and Poo M M 1998 *J. Neurosci.* **18** 10464
[36] Debanne D, Gähwiler B H and Thompson S M 1998 *J. Physiol.* **507** 237
[37] Caporale N and Dan Y 2008 *Annu. Rev. Neurosci.* **31** 25
[38] Froemke R, Poo M M and Dan Y 2005 *Nature* **434** 221
[39] Rodríguez-Moreno A and Paulsen O 2008 *Nat. Neurosci.* **11** 744
[40] Li X, Sun J, Sun Y and Zhang J 2024 *Nonlinear Dyn.* **113** 3763
[41] Sun J, Sun J, Li X, Sun Y, Hong Q and Wang C 2025 *Nonlinear Dyn.* **113** 33035